Clinical Radiology 74 (2019) 973.e1–973.e6

Contents lists available at ScienceDirect

Clinical Radiology

journal homepage: www.clinicalradiologyonline.net

Diagnostic performance of a fast non-invasive fractional flow reserve derived from coronary CT angiography: an initial validation study

L. Yang [a], L. Xu [a,*], J. He [b], Z. Wang [b], Z. Sun [c], Z. Fan [a], Y. Huo [d,e], Y. Zhou [b]

[a] *Department of Radiology, Beijing Anzhen Hospital, Capital Medical University, 2 Anzhen Rd Chaoyang District, Beijing, 100029, China*
[b] *Department of Cardiology, Beijing Anzhen Hospital, Capital Medical University, 2 Anzhen Rd Chaoyang District, Beijing, 100029, China*
[c] *Department of Medical Radiation Sciences, Curtin University, Perth, WA, 6845, Australia*
[d] *PKU-HKUST Shenzhen-Hongkong Institution, Shenzhen, 518057, China*
[e] *Department of Mechanics and Engineering Science, College of Engineering, Peking University, 298 Chengfu Rd, Haidian District, Beijing, 100871, China*

ARTICLE INFORMATION

Article history:
Received 7 August 2018
Accepted 19 August 2019

AIM: To validate the computed tomography (CT)-derived fractional flow reserve (FFR_{CT}) that was computed by new, fast, automatic software and to compare the diagnostic accuracy between FFR_{CT} and stenosis diagnosed at coronary CT angiography (CCTA).

MATERIALS AND METHODS: A total of 110 patients (76 males, 59±9 years) and 125 vessels underwent CCTA. FFR_{CT} was computed by fast automatic software and compared with invasive FFR. The diagnostic performance between FFR_{CT} and CCTA-diagnosed stenosis were compared on the per-patient and per-vessel level.

RESULTS: The computational time of FFR_{CT} is 10±5 minutes (averaged over 125 vessels). The FFR_{CT} has a good correlation with invasive FFR (r=0.59, p<0.0001) with a small bias of −0.02 (−0.26–0.23). The sensitivity, specificity, positive predictive value (PPV), and negative predictive value (NPV) of FFR_{CT} were 76.5, 89.5, 89.7, and 76.1% on a vessel level. The area under the receiver operating characteristic curve of FFR_{CT} was higher than CCTA-diagnosed stenosis (0.82 versus 0.72, P=0.034).

CONCLUSION: The computation of FFR_{CT} is possible and reliable when using the new, fast, automatic software first employed in the present clinical study. The FFR_{CT} has a good correlation with invasive FFR and provides better diagnostic performance than CCTA-diagnosed stenosis.

Introduction

Although coronary computed tomography (CT) angiography (CCTA) has been established as an effective non-invasive method for anatomical assessment of coronary

* Guarantor and correspondent: Lei Xu, Department of Radiology, Beijing Anzhen Hospital, Capital Medical University, 2 Anzhen Rd, Chaoyang District, Beijing, 100029, China. Tel.: +86 10 64456071; fax: +86 10 64456310.
E-mail address: leixu2001@hotmail.com (L. Xu).

https://doi.org/10.1016/j.crad.2019.08.007
0009-9260/

artery disease (CAD),[1,2] there is still lack of sufficient evidence of CCTA-determined guidance for myocardial ischaemia.[3] Invasive coronary angiography in conjunction with fractional flow reserve (FFR) is the current reference standard for ischaemic evaluation and therapeutic decision-making in patients with CAD.[4,5] Conversely, studies have prompted concern that the utilisation of CCTA may result in an increase in inappropriate downstream referrals to coronary angiography.[6,7] This requires more accurate non-invasive gatekeeping approaches to the catheterisation laboratory beyond anatomical assessment using CCTA.[8,9]

Some non-invasive cardiac tests, e.g., single-photon-emission CT (SPECT), cardiac magnetic resonance imaging (CMRI), and stress echocardiography, have been recommended for functional diagnosis of CAD according to ACCF/AHA/SCAI guidelines for PCI.[10] On a per-vessel analysis, these methods do not, however, visualise coronary stenoses and provide accurate haemodynamic information of coronary lesions compared with invasive FFR, particularly in patients with balanced ischaemia.[1,11–13] Owing to the rapid development of computational fluid dynamics (CFD), FFR derived from CCTA (FFR_{CT}), has been investigated extensively.[14–17] FFR_{CT} is a promising non-invasive approach for the diagnosis of coronary stenosis severity because it allows detection of lesion-specific ischaemia.[16] The diagnostic performance of FFR_{CT} has been shown to be superior to CCTA alone for coronary stenotic assessment even in patients and vessels with a high Agatston score.[17–19]

In the present study, the diagnostic performance of FFR_{CT} computed by new, fast, automatic software, which was first employed in the present clinical study, was validated and compared with invasive FFR measurements.

Materials and methods

Study population

The present retrospective study analysed 110 patients who underwent CCTA for evaluation of CAD and underwent a subsequent invasive coronary angiography examination and FFR measurement. All patients underwent CCTA <30 days before invasive coronary angiography. The exclusion criteria for quantitative CT data analysis included restenosis in coronary stents (four cases), stenosis caused by myocardial bridge (two cases), and Digital Imaging and Communications in Medicine (DICOM) data unrecognised by the software (four cases). Finally, 100 patients (a total of 125 vessels) were included in the study. FFR_{CT} and stenosis were assessed in each vessel with regard to the invasive FFR. The study protocol was approved by the Institutional Review Board. Patient informed consent was waived due to the retrospective nature of the study.

CCTA image acquisition

CCTA was performed on three different CT systems, i.e., 256-detector row CT (Revolution CT, GE Healthcare, Milwaukee, WI, USA), 320-detector row CT (Aquilion One; Toshiba, Otawara, Japan), or 64-detector row dual-source CT systems (Somatom Definition Flash; Siemens, Forchheim, Germany), according to the guidelines of the Society of Cardiovascular Computed Tomography.[20] The CCTA images were acquired when 50–60 ml contrast agent (370 mg iodine/ml, Ultravist, Bayer Schering Pharma, Berlin, Germany) was injected at a rate of 4.5–5 ml/s followed by intravenous injection of saline chasing of 30–35 ml at a rate of 5 ml/s, similar to a previous study.[21]

Prospective electrocardiography gating and bolus tracking were used for CCTA image acquisition. Gantry rotation time was in the range of 0.28–0.35 seconds per rotation, depending on the CT system used. A tube voltage of 100 or 120 kV with automatically selected tube current was applied for image acquisition while transaxial images were reconstructed with 0.5, 0.6, or 0.625 mm section thickness. The position of the reconstruction window within the cardiac cycle was individually selected to minimise artefacts. Motion-free data sets were collected for analysis. All images were considered diagnostic image quality with optimal contrast enhancement and no substantial motion artefacts.

Coronary arteries and branches are categorised into 1 of 4 vascular territories: left main (LM) artery, left anterior descending (LAD) artery, left circumflex (LCX) artery, and right coronary artery (RCA). Diagonal branches, obtuse marginal branches, and posterolateral branches were considered primary branches of the LAD, LCX, and RCA, respectively. The posterior descending artery was considered part of the RCA or LCX system, depending upon the coronary artery dominance.

Quantification of coronary stenosis and FFR from CCTA

Non-invasive FFR_{CT} analysis was carried out by independent blinded researchers using commercial software (Auto vessel 1.0, RunXin Co., Suzhou, China) installed in a local computing environment. Three-dimensional (3D) geometrical model of an epicardial coronary arterial tree was constructed after loading the motion-free CT images. The centreline and contour of vessels were processed automatically. Manual adjustments were performed if necessary. The quantitative percentage of stenosis was calculated by dividing the narrowest lumen diameter of stenosis by the mean of two healthy, non-diseased reference points (Fig 1c and d). Severe stenosis was defined as ≥50% in reference points with diameter ≥2 mm. Briefly, the flow rates at the inlet of LM artery and RCA were estimated from the CT-determined myocardial size and the outlet flow velocities were determined based on the scaling law[22] (see details in the Electronic Supplementary Material Appendix). Based on the outlet flow velocities, the flow rate in the epicardial coronary arterial tree was computed using a finite element solver (C++ programming) similar to a previous study.[23] The pressure gradient (ΔP) was calculated through stenosis. FFR was determined as $\frac{P_a-\Delta P}{P_a}$, where P_a is the mean aortic pressure[24] (see details in the Electronic Supplementary Material Appendix). FFR_{CT} ≤0.80 was considered the diagnosis of lesion-specific ischaemia.[16]

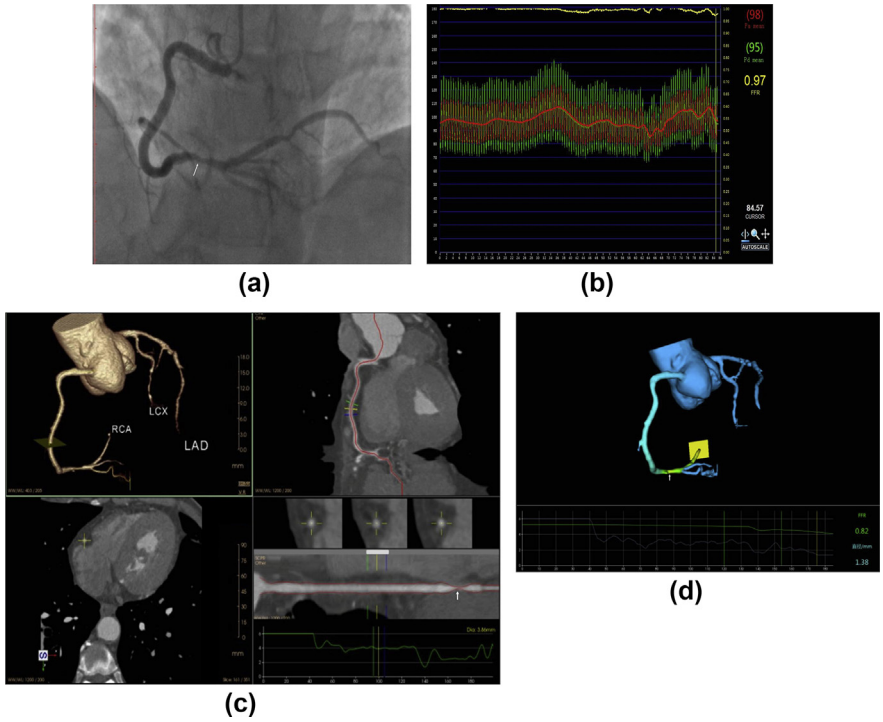

Figure 1 Example of a representative patient with no significant coronary stenosis. A patient with atypical chest pain, hypertension, hyperlipidaemia, and smoking history. (a) Invasive coronary angiography shows moderate stenosis (50–70%) in the distal segment of right coronary artery (RCA; white arrow). (b) Invasive FFR showing 0.97 of the RCA. (c–d) FFR_{CT} analysis indicates that the RCA lesions are not haemodynamically significant, with FFR_{CT} in the RCA of 0.82.

Invasive measurement of FFR

Selective invasive coronary angiography and FFR were performed under standard practice[25] (Fig 1a and b). The pressure-wire was positioned in a vessel segment ≥2 mm that was 20–30 mm distal to a stenosis. Hyperaemia was induced by intravenous injection of adenosine (140–180 μg/kg/min). Interventional cardiologists performed the FFR measurements according to standard guidelines.

Statistical analysis

Continuous variables are presented as means ± standard deviation (SD) or medians (interquartile range) as appropriate, and categorical variables as numbers and percentages. The sensitivity, specificity, positive predictive value (PPV), and negative predictive value (NPV) were determined. The Bland–Altman analysis and the Pearson correlation coefficient analysis were performed to evaluate the variation and agreement between FFR_{CT} and invasive FFR. A comparison of receiver operating characteristic (ROC) curves was performed by using DeLong test. The area under the ROC curve (AUC) was employed to evaluate the discrimination of ischaemia from the FFRCT.[26] A p-value of ≤0.05 represented a statistically significant difference. Statistical analyses were performed using MedCalc software (version 15; MedCalc Software BVBA, Ostend, Belgium) and SPSS17.0 software (SPSS, Chicago, IL, USA).

Results

A total of 100 patients (24 females) with 125 stenotic vessels underwent invasive FFR and FFR_{CT} examinations. This includes 84 LAD arteries and diagonal branches (67.2%), 19 LCX arteries (15.2%) and 22 RCAs (17.6%). Table 1 lists the baseline characteristics of these patients with mean ages of 59±8.9 years and BMI of 26.1±3.3 kg/m^2. Moreover, the results of stenosis and FFR_{CT} derived from CCTA, and invasive FFR are listed in Table 2. According to CCTA images, there were four lesions with <50% stenosis, 45 lesions with ≥70% stenosis, and 76 lesions with moderate stenosis.

The computational time of FFR_{CT} including CTA data loading to computation has mean±SD values of 10±5 minutes (averaged over 125 vessels). The relationship between FFR_{CT} and invasive FFR is illustrated in Fig 2a. Bland–Altman

Table 1
Demographics of the study population

Variable (n=100)	Mean± SD or frequency (%)
Age, mean ± SD (years)	59.15±8.9
Male/Female gender	76/24
BMI, mean ± SD (kg/m^2)	26.13±3.3
Diabetes mellitus	29
Hypertension	61
Hyperlipidaemia	42
Current smoker	43
Current drinker	21

SD, standard deviation.

Table 2
Determination of coronary artery disease by Stenosis, FFR_{CT} and FFR

	Patient level (n=100)		Vessel level (n=125)	
	FFR≤0.8	FFR>0.8	FFR≤0.8	FFR>0.8
FFR_{CT} ≤0.8	46	6	52	6
FFR_{CT} >0.8	8	40	16	51
CTA stenosis ≥50%	55	42	68	53
CTA stenosis <50%	0	3	0	4

analysis shows the mean difference of −0.02 (−0.26–0.23; Fig 2b).

In comparison with invasive FFR measurements, the diagnostic accuracy of FFR_{CT} was evaluated with a sensitivity of 76.5%, specificity of 89.5%, PPV of 89.7%, and NPV of 76.1% on vessel level. The diagnostic accuracy and AUC (ROC) were significantly different between FFR_{CT} and CCTA-diagnosed stenosis severity on the vessel and patient level.

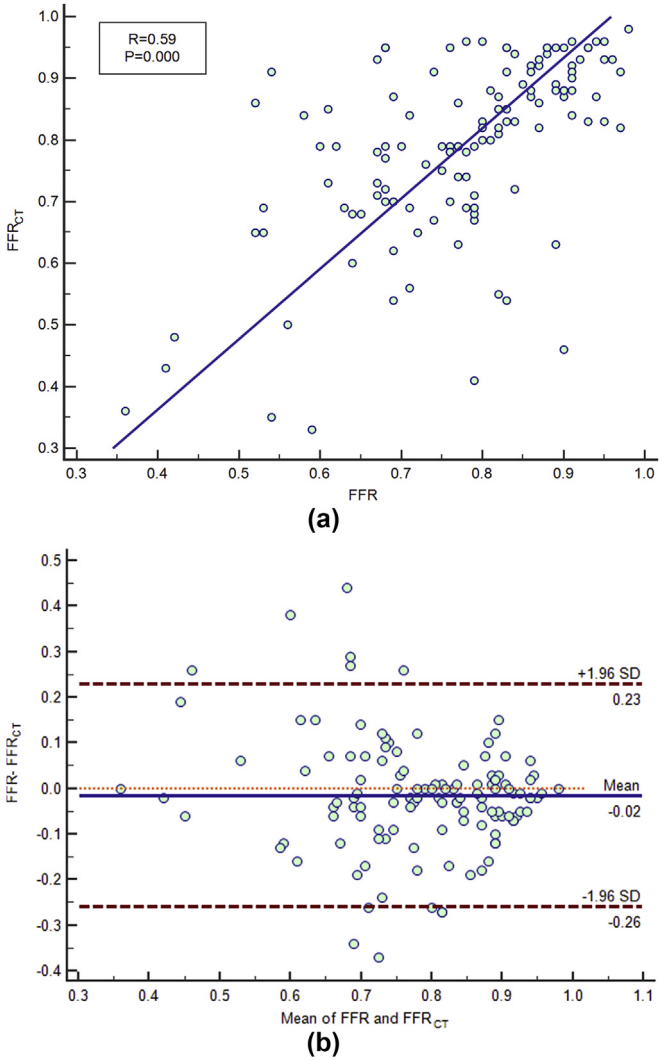

Figure 2 Correlation and Bland–Altman plot of FFR_{CT} to invasive FFR. Per-vessel correlation of FFR_{CT} versus FFR (a) shows r=0.59 (p<0.0001) and Bland–Altman plots of FFR_{CT} versus FFR (b) indicates the mean difference −0.02 (−0.26–0.23).

The AUCs (95% CI) for discrimination of ischaemia (obtained from invasive FFR ≤0.80) were 0.72 (0.63–0.79) by CCTA-diagnosed diameter stenosis ≥50% and 0.82 (0.74–0.88) by FFR_{CT} ≤0.80 (p=0.034) on a vessel level, as shown in Table 3 and Fig 3.

Discussion

The present study examined the diagnostic performance of FFR_{CT} using new, fast, automatic software in comparison with invasive FFR measurements. Moreover, the diagnostic accuracy of FFR_{CT} was compared with the performance of CCTA-diagnosed stenosis alone. The major findings of the study were that[1] the computation of FFR_{CT} by this new software is possible,[2] the FFR_{CT} has good correlation with invasive FFR, and[3] the FFR_{CT} provides better diagnostic performance than CCTA-diagnosed stenosis.

The high computational demand of FFR_{CT} limited the clinical application in previous studies (e.g., the DISCOVER-FLOW study).[16] Some methods have been proposed to reduce the computation time of FFR_{CT}.[27–31] For example, De Geer *et al.* analysed 21 patients with 23 vessels to show the on-site efficient computation of FFR_{CT}.[31] The mean times for FFR_{CT} and complete FFR_{CT} post-processing was 3 minutes 28 seconds and 45 minutes, respectively, which are much shorter than that with off-site estimation at the HeartFlow core laboratory (~24 hours). The present model and other FFR_{CT} techniques (e.g., FFR_{CT} from HeartFlow Inc.) used the CFD method to solve continuity and Navier–Stokes equations for the computation of pressure drop across stenosis. FFR_{CT} from HeartFlow Inc. required the coupling lumped parameter models of the heart, systemic circulation, and coronary microcirculation as the outlet boundary conditions.[16] Patient-specific MAP was set to the boundary condition at the inlet of epicardial coronary arterial tree; however, the present model used the flow velocity at each outlet as the boundary condition. There were utterly different boundary conditions between the present model and FFR_{CT} from HeartFlow Inc. Hence, the present model significantly reduced the computational time (~10 minutes per case) as compared with FFR_{CT} from HeartFlow Inc. and other methods that reported in previous studies (from 30 minutes to 3 hours).[16,29–31] All image processing and interpretation were performed through commercial software (Auto Vessel 1.0, RunXin Co., Suzhou, China) and the user can easily view the stenosis and FFR_{CT} of each coronary artery.

The present study validated the diagnostic performance of FFR_{CT} compared with invasive FFR. There was a statistical correlation between FFR_{CT} values and invasive FFR results (r=0.59), while the Bland–Altman analysis revealed a small bias of −0.02 (−0.26–0.23). It indicates that this new fast software may make a safely computational result of FFR_{CT}. In the present study, the performance of diagnosis of ischaemic lesions was further compared with CCTA-determined stenosis alone. The overall diagnostic accuracy and AUC for FFR_{CT} were much better than those for CCTA-determined stenosis alone. The sensitivity, specificity, PPV,

Table 3
Performance of diagnosing ischaemia of coronary stenosis severity and FFR_{CT}

	Patient level (n=100)		Vessel level (n=125)	
	FFR_{CT}	Stenosis severity	FFR_{CT}	Stenosis severity
Sensitivity (95% CI)	85.2 (72.3–92.9)	100 (91.9–100)	76.5 (64.4–85.6)	100 (93.3–100)
Specificity (95% CI)	87.0 (73–94.6)	6.7 (1.7–19.3)	89.5 (77.8–95.6)	7 (2.3–17.8)
PPV (95% CI)	88.5 (75.9–95.2)	56.7 (46.3–66.7)	89.7 (78.2–95.7)	56.2 (46.9–65.1)
NPV (95% CI)	83.3 (69.2–92)	100 (31–100)	76.1 (63.9–85.3)	100 (39.6–100)
AUC (ROC) (95% CI)	0.89 (0.81–0.94)	0.76 (0.67–0.85)	0.82 (0.74–0.88)	0.72 (0.63–0.79)

Values are % (n/N).
NPV, negative predictive value; PPV, positive predictive value; AUC, area under the curve; ROC, receiver operating characteristic; CI, confidence interval.

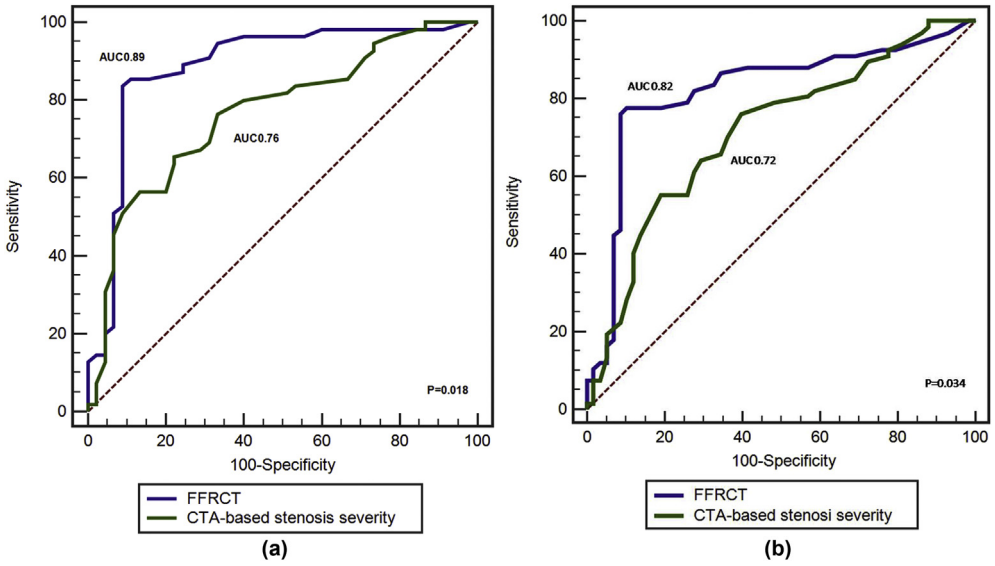

Figure 3 ROC curves of CCTA-based stenosis severity and FFR_{CT} for diagnosis of the ischaemia. Discrimination of ischaemia by FFR_{CT} (≤0.80) and CCTA (lumen reduction ≥50%) on patient level (a) and vessel level (b).

and NPV in the present study values were 76.5%, 89.5%, 89.7%, and 76.1% on a vessel level. The specificity of FFR_{CT} was high and the sensitivity is moderate as compared with invasive FFR. FFR_{CT} improved the diagnostic specificity of CCTA consistent with previous multicentre studies.[16,17,32] This further highlights the improved performance of using FFR_{CT} compared to CCTA alone. The PLATFORM trial demonstrated that the addition FFR_{CT} to CCTA increased the diagnostic certainty given cancellation of 61% of invasive coronary angiography in patients who were initially planned for an invasive procedure.[33] This study supported the conclusion that the FFR_{CT} could reduce the healthcare cost for patients suspected of having CAD at the same time.

Because the 3D geometrical model of the coronary arterial tree derived from CT images was used, the spatial resolution in the small-diameter vessels of CCTA could result in deviation between reconstructed geometries and actual anatomy, contributing bias to the stenosis and FFR_{CT} computation. As this study focused on coronary stenoses of moderate and severe size, the relationship between stenoses of various sizes, plaque features, and functional severity with FFR-CT and invasive FFR should be analysed in future studies. Patients with previous percutaneous coronary intervention or bypass surgery were not included in the study. The present FFR_{CT} software will be applied to these patients in ongoing investigations.

In this clinical study, a fast and simplified tool was used to compute FFR derived from CCTA data. It provided good diagnostic performance of FFR_{CT} compared with invasive FFR and improved the performance of CCTA in diagnosing ischaemia.

Conflicts of interest

The authors declare no conflict of interest.

Acknowledgements

This study was supported by a grant from the National Key R&D Program of China (2016YFC1300301) and a grant from the National Natural Science Foundation of China (81641069).

Appendix A. Supplementary data

Supplementary data to this article can be found online at https://doi.org/10.1016/j.crad.2019.08.007.

References

1. Alani A, Nakanishi R, Budoff MJ. Recent improvement in coronary computed tomography angiography diagnostic accuracy. *Clin Cardiol* 2014;**37**:428–33. https://doi.org/10.1002/clc.22286.
2. American College of Cardiology Foundation Task Force on Expert Consensus D, Mark DB, Berman DS, *et al*. ACCF/ACR/AHA/NASCI/SAIP/SCAI/SCCT 2010 expert consensus document on coronary computed tomographic angiography: a report of the American College of Cardiology Foundation Task Force on Expert Consensus Documents. *Circulation* 2010;**121**:2509–43. https://doi.org/10.1161/CIR.0b013e3181d4b618.
3. Doh JH, Koo BK, Nam CW, *et al*. Diagnostic value of coronary CT angiography in comparison with invasive coronary angiography and intravascular ultrasound in patients with intermediate coronary artery stenosis: results from the prospective multicentre FIGURE-OUT (Functional Imaging criteria for GUiding REview of invasive coronary angiography, intravascular Ultrasound, and coronary computed Tomographic angiography) study. *Eur Heart J Cardiovasc Imaging* 2014;**15**:870–7. https://doi.org/10.1093/ehjci/jeu009.
4. Pijls NH, Fearon WF, Tonino PA, *et al*. Fractional flow reserve versus angiography for guiding percutaneous coronary intervention in patients with multivessel coronary artery disease: 2-year follow-up of the FAME (Fractional Flow Reserve versus Angiography for Multivessel Evaluation) study. *J Am Coll Cardiol* 2010;**56**:177–84. https://doi.org/10.1016/j.jacc.2010.04.012.
5. Tonino PA, De Bruyne B, Pijls NH, *et al*. Fractional flow reserve versus angiography for guiding percutaneous coronary intervention. *N Engl J Med* 2009;**360**:213–24. https://doi.org/10.1056/NEJMoa0807611.
6. Redberg RF, Walsh P. Pay now, benefits may follow—the case of cardiac computed tomography. *N Engl J Med* 2008;**359**:2309–11. https://doi.org/10.1056/NEJMp0805920.
7. Shreibati JB, Baker LC, Hlatky MA. Association of coronary CT angiography or stress testing with subsequent utilisation and spending among Medicare beneficiaries. *JAMA* 2011;**306**:2128–36. https://doi.org/10.1001/jama.2011.1652.
8. Patel MR. Detecting obstructive coronary disease with CT angiography and non-invasive fractional flow reserve. *JAMA* 2012;**308**:1269–70. https://doi.org/10.1001/2012.jama.11383.
9. Meijboom WB, Van Mieghem CA, van Pelt N, *et al*. Comprehensive assessment of coronary artery stenoses: computed tomography coronary angiography versus conventional coronary angiography and correlation with fractional flow reserve in patients with stable angina. *J Am Coll Cardiol* 2008;**52**:636–43. https://doi.org/10.1016/j.jacc.2008.05.024.
10. Levine GN, Bates ER, Blankenship JC, *et al*. 2011 ACCF/AHA/SCAI guideline for percutaneous coronary intervention: a report of the American college of cardiology foundation/American heart association task force on practice guidelines and the society for cardiovascular angiography and interventions. *Catheter Cardiovasc Interv* 2013;**82**:E266–355. https://doi.org/10.1002/ccd.23390.
11. Gotberg M, Cook CM, Sen S, *et al*. The evolving future of instantaneous wave-free ratio and fractional flow reserve. *J Am Coll Cardiol* 2017;**70**:1379–402. https://doi.org/10.1016/j.jacc.2017.07.770.
12. Min JK, Shaw LJ, Berman DS. The present state of coronary computed tomography angiography a process in evolution. *J Am Coll Cardiol* 2010;**55**:957–65. https://doi.org/10.1016/j.jacc.2009.08.087.
13. Berman DS, Kang X, Slomka PJ, *et al*. Underestimation of extent of ischaemia by gated SPECT myocardial perfusion imaging in patients with left main coronary artery disease. *J Nucl Cardiol* 2007;**14**:521–8. https://doi.org/10.1016/j.nuclacrd.2007.05.008.
14. Koo BK, Erglis A, Doh JH, *et al*. Diagnosis of ischaemia-causing coronary stenoses by non-invasive fractional flow reserve computed from coronary computed tomographic angiograms. Results from the prospective multicenter DISCOVER-FLOW (Diagnosis of Ischaemia-Causing Stenoses Obtained via Noninvasive Fractional Flow Reserve) study. *J Am Coll Cardiol* 2011;**58**:1989–97. https://doi.org/10.1016/j.jacc.2011.06.066.
15. Min JK, Leipsic J, Pencina MJ, *et al*. Diagnostic accuracy of fractional flow reserve from anatomic CT angiography. *JAMA* 2012;**308**:1237–45. https://doi.org/10.1001/2012.jama.11274.
16. Taylor CA, Fonte TA, Min JK. Computational fluid dynamics applied to cardiac computed tomography for noninvasive quantification of fractional flow reserve scientific basis. *J Am Coll Cardiol* 2013;**61**:2233–41. https://doi.org/10.1016/j.jacc.2012.11.083.
17. Coenen A, Lubbers MM, Kurata A, *et al*. Fractional flow reserve computed from non-invasive CT angiography data: diagnostic performance of an on-site clinician-operated computational fluid dynamics algorithm. *Radiology* 2015;**274**:674–83. https://doi.org/10.1148/radiol.14140992.
18. Ko BS, Cameron JD, Munnur RK, *et al*. Noninvasive CT-derived FFR based on structural and fluid analysis: a comparison with invasive FFR for detection of functionally significant stenosis. *JACC Cardiovasc Imaging* 2017;**10**:663–73. https://doi.org/10.1016/j.jcmg.2016.07.005.
19. Norgaard BL, Gaur S, Leipsic J, *et al*. Influence of coronary calcification on the diagnostic performance of CT angiography derived FFR in coronary artery disease: a substudy of the NXT Trial. *JACC Cardiovasc Imaging* 2015;**8**:1045–55. https://doi.org/10.1016/j.jcmg.2015.06.003.
20. Weigold WG, Abbara S, Achenbach S, *et al*. Standardized medical terminology for cardiac computed tomography: a report of the Society of Cardiovascular Computed Tomography. *J Cardiovasc Comput Tomogr* 2011;**5**:136–44. https://doi.org/10.1016/j.jcct.2011.04.004.
21. Huo Y, Wischgoll T, Choy JS, *et al*. CT-based diagnosis of diffuse coronary artery disease on the basis of scaling power laws. *Radiology* 2013;**268**:694–701. https://doi.org/10.1148/radiol.13122181.
22. Fan T, Lu Y, Gao Y, *et al*. Hemodynamics of left internal mammary artery bypass graft: effect of anastomotic geometry, coronary artery stenosis, and postoperative time. *J Biomech* 2016;**49**:645–52. https://doi.org/10.1016/j.jbiomech.2016.01.031.
23. Huo Y, Li BQ. Three-dimensional Marangoni convection in electrostatically positioned droplets under microgravity. *Int J Heat Mass Transf* 2004;**47**:3533–47. https://doi.org/10.1016/j.ijheatmasstransfer.2004.01.021.
24. Huo Y, Svendsen M, Choy JS, *et al*. A validated predictive model of coronary fractional flow reserve. *J R Soc Interface* 2012;**9**:1325–38. https://doi.org/10.1098/rsif.2011.0605.
25. van de Hoef TP, Nolte F, Damman P, *et al*. Diagnostic accuracy of combined intracoronary pressure and flow velocity information during baseline conditions: adenosine-free assessment of functional coronary lesion severity. *Circ Cardiovasc Interv* 2012;**5**:508–14. https://doi.org/10.1161/CIRCINTERVENTIONS.111.965707.
26. Greiner M, Sohr D, Gobel P. A modified ROC analysis for the selection of cut-off values and the definition of intermediate results of serodiagnostic tests. *J Immunol Methods* 1995;**185**:123–32. https://doi.org/10.1016/0022-1759 (95)00121-.
27. Tesche C, De Cecco CN, Baumann S, *et al*. Coronary CT angiography-derived fractional flow reserve: machine learning algorithm versus computational fluid dynamics modeling. *Radiology* 2018;**288**:64–72. https://doi.org/10.1148/radiol.2018171291.
28. Yang DH, Kim YH, Roh JH, *et al*. Diagnostic performance of on-site CT-derived fractional flow reserve versus CT perfusion. *Eur Heart J Cardiovasc Imaging* 2017;**18**:432–40. https://doi.org/10.1093/ehjci/jew094.
29. Zhang JM, Zhong L, Luo T, *et al*. Simplified models of non-invasive fractional flow reserve based on CT images. *PloS One* 2016;**11**:e0153070, https://doi.org/10.1371/journal.pone.0153070.
30. Chung JH, Lee KE, Nam CW, *et al*. Diagnostic performance of a novel method for fractional flow reserve computed from noninvasive computed tomography angiography (NOVEL-FLOW Study). *Am J Cardiol* 2017;**120**:362–8. https://doi.org/10.1016/j.amjcard.2017.04.057.
31. De Geer J, Sandstedt M, Bjorkholm A, *et al*. Software-based on-site estimation of fractional flow reserve using standard coronary CT angiography data. *Acta Radiol* 2016;**57**:1186–92. https://doi.org/10.1177/0284185115622075.
32. Norgaard BL, Leipsic J, Gaur S, *et al*. Diagnostic performance of non-invasive fractional flow reserve derived from coronary computed tomography angiography in suspected coronary artery disease: the NXT trial (Analysis of Coronary Blood Flow Using CT Angiography: next Steps). *J Am Coll Cardiol* 2014;**63**:1145–55. https://doi.org/10.1016/j.jacc.2013.11.043.
33. Douglas PS, Pontone G, Hlatky MA, *et al*. Clinical outcomes of fractional flow reserve by computed tomographic angiography-guided diagnostic strategies vs. usual care in patients with suspected coronary artery disease: the prospective longitudinal trial of FFR (CT): outcome and resource impacts study. *Eur Heart J* 2015;**36**:3359–67. https://doi.org/10.1093/eurheartj/ehv444.